Author Manuscript

Author Manuscript

Author Manuscript

Author Manuscript

HHS Public Access

Author manuscript

Oncogene. Author manuscript; available in PMC 2013 December 20.

Published in final edited form as:

Oncogene. 2013 June 20; 32(25): 3091–3100. doi:10.1038/onc.2012.315.

Mutations in *Isocitrate Dehydrogenase 1* and *2* Occur Frequently in Intrahepatic Cholangiocarcinomas and Share Hypermethylation Targets with Glioblastomas

Pu Wang[1,2,$], **Qiongzhu Dong**[3,$], **Chong Zhang**[4], **Pei-Fen Kuan**[5,6], **Yufeng Liu**[4], **William R. Jeck**[6,7], **Jesper B. Andersen**[8], **Wenqing Jiang**[1,2], **Gleb L. Savich**[6,7], **Ting-Xu Tan**[6,7], **J. Todd Auman**[6,9], **Janelle M. Hoskins**[6,9], **Anne D. Misher**[6,9], **Catherine D. Moser**[10], **Scott M. Yourstone**[6,7], **Jin Woo Kim**[11], **Kristian Cibulskis**[12], **Gad Getz**[12], **Heike V. Hunt**[13], **Snorri S. Thorgeirsson**[8], **Lewis R. Roberts**[10], **Dan Ye**[2], **Kun-Liang Guan**[1,2,14,15], **Yue Xiong**[1,2,6,16,17], **Lun-Xiu Qin**[3,17], and **Derek Y. Chiang**[6,7,17]

[1]State Key Lab of Genetic Engineering, School of Life Sciences, Fudan University, Shanghai 200032, China

[2]Molecular and Cell Biology Lab, Institutes of Biomedical Sciences, Fudan University, Shanghai 200032, China

[3]Liver Cancer Institute and Zhongshan Hospital, Institutes of Biomedical Sciences, Fudan University, Shanghai 200032, China

[4]Department of Statistics and Operations Research and Carolina Center for Genome Sciences, University of North Carolina, Chapel Hill, NC 27599 USA

[5]Department of Biostatistics, University of North Carolina, Chapel Hill, NC 27599 USA

[6]Lineberger Comprehensive Cancer Center, University of North Carolina, Chapel Hill, NC 27599 USA

[7]Department of Genetics, University of North Carolina, Chapel Hill, NC 27599 USA

[8]Laboratory of Experimental Carcinogenesis, Center for Cancer Research, National Cancer Institute, National Institutes of Health, Bethesda, MD 20892-4262, USA

[9]Institute of Pharmacogenomics and Individualized Medicine, University of North Carolina, Chapel Hill, NC 27599 USA

[10]Division of Gastroenterology and Hepatology, Mayo Clinic Center for Cell Signaling in Gastroenterology and Mayo Clinic Cancer Center, Mayo Clinic, Rochester, MN 55905, USA

Users may view, print, copy, download and text and data- mine the content in such documents, for the purposes of academic research, subject always to the full Conditions of use: http://www.nature.com/authors/editorial_policies/license.html#terms

[17]Corresponding Authors: Derek Y. Chiang & Yue Xiong, Lineberger Cancer Center, CB #7295, 450 West Drive, Chapel Hill, NC 27599, (919) 843-7887, (919) 962-2142, chiang@med.unc.edu, yxiong@email.unc.edu. Lun-Xiu Qin, Liver Cancer Institute & Zhongshan Hospital, 180 Feng Lin Road, Shanghai 200032, China, 86-21-5423-7960, qin.lunxiu@zs-hospital.sh.cn.

[$]These authors contributed equally

POTENTIAL CONFLICTS OF INTEREST

D.Y.C. is a consultant for Aveo Pharmaceuticals and Entremed, and held minor stock ownership in Illumina, which did not have any role in the study design, data collection and analysis, decision to publish, or preparation of the manuscript.

Author Manuscript Author Manuscript Author Manuscript Author Manuscript

[11]Center for Cancer Genomics, Wake Forest University Baptist Medical Center, Winston-Salem, NC 27157

[12]Genome Sequencing Analysis Program and Platform, Broad Institute, 7 Cambridge Center, Cambridge, MA 02142, USA

[13]Department of Pathology and Laboratory Medicine, University of North Carolina, Chapel Hill, NC 27599 USA

[14]Department of Biochemistry, Shanghai Medical College, Fudan University, Shanghai 200032, China

[15]Department of Pharmacology and Moores Cancer Center, University of California San Diego, La Jolla, CA 92093

[16]Department of Biochemistry and Biophysics, University of North Carolina, Chapel Hill, NC 27599 USA

Abstract

Mutations in the genes encoding isocitrate dehydrogenase, *IDH1* and *IDH2*, have been reported in gliomas, myeloid leukemias, chondrosarcomas, and thyroid cancer. We discovered *IDH1* and *IDH2* mutations in 34 of 326 (10%) intrahepatic cholangiocarcinomas. Tumor with mutations in *IDH1* or *IDH2* had lower 5-hydroxymethylcytosine (5hmC) and higher 5-methylcytosine (5mC) levels, as well as increased dimethylation of histone H3K79. Mutations in *IDH1* or *IDH2* were associated with longer overall survival ($p = 0.028$) and were independently associated with a longer time to tumor recurrence after intrahepatic cholangiocarcinoma resection in multivariate analysis ($p = 0.021$). *IDH1* and *IDH2* mutations are significantly associated with increased levels of p53 in intrahepatic cholangiocarcinomas, but no mutations in the *p53* gene were found, suggesting that mutations in *IDH1* and *IDH2* may cause a stress that leads to p53 activation. We identified 2,309 genes that were significantly hypermethylated in 19 cholangiocarcinomas with mutations in *IDH1* or *IDH2*, compared with cholangiocarcinomas without these mutations. Hypermethylated CpG sites were significantly enriched in CpG shores and upstream of transcription start sites, suggesting a global regulation of transcriptional potential. Half of the hypermethylated genes overlapped with DNA hypermethylation in *IDH1*-mutant gliobastomas, suggesting the existence of a common set of genes whose expression may be affected by mutations in *IDH1* or *IDH2* in different types of tumors.

Keywords

DNA methylation; Epigenetics; Tumor metabolism

INTRODUCTION

IDH1 and *IDH2* encode the $NADP^+$-dependent isocitrate dehydrogenase, localizing to the cytoplasm and mitochondria, respectively, and catalyze the oxidative decarboxylation of isocitrate to produce α-ketoglutarate (α-KG). *IDH1* and *IDH2* represent the most frequently mutated metabolic genes in human cancer, mutated in more than 75% of low grade gliomas

Author Manuscript Author Manuscript Author Manuscript Author Manuscript

and secondary glioblastoma multiforme (GBM), 20% of acute myeloid leukemia (AML), 56% of chondrosarcomas, over 80% of Ollier disease and Maffucci syndrome, and 10% of melanoma (1–6). Tumor mutations targeting *IDH1* and *IDH2* cause simultaneous loss and gain of activities in the production of α-KG and 2-hydroxyglutarate (2-HG), respectively (7, 8). It was recently demonstrated that 2-HG functions as an α-KG antagonist by binding to the same space in the catalytic site and competitively inhibiting the activity of α-KG-dependent dioxygenases, including α-KG-dependent histone demethylases and the TET family of 5-methylcytosine hydroxylases. Thus, *IDH1* and *IDH2* mutations would be predicted to alter histone and DNA methylation in both cultured cells and primary gliomas (9). This model is supported by the finding that the mutations of *IDH1* and *IDH2* genes occur in a mutually exclusive manner with that of *TET2* gene in acute myeloid leukemias (10).

The TET family of α-KG-dependent dioxygenases catalyzes the sequential oxidation of 5-methylcytosine (5mC) to 5-hydroxymethylcytosine (5hmC), 5-formylcytosine (5fC), and 5-carboxylcytosine (5caC), leading to eventual DNA demethylation (11–14). Tumors with *IDH1* or *IDH2* mutations would be predicted to have lower TET enzymatic activity, and thus accumulate DNA methylation. Indeed, glioblastomas with *IDH1* mutations exhibited a CpG Island Methylator Phenotype (15) and belonged to a proneural gene expression class with increased *PDGFR* gene expression and *TP53* mutation (16). These molecular correlates suggest that *IDH1* mutations may represent early events in the pathogenesis of low-grade gliomas and secondary glioblastomas (1, 17).

The CpG Island Methylator Phenotype was originally described in colorectal cancer, and has subsequently been associated with mutations in *BRAF* (18, 19). Promoter hypermethylation and concomitant silencing of tumor suppressor genes – such as *p16*, *MLH1* and *BRCA1* – can accelerate tumor progression (20). Certain genomic regions are more prone to increased methylation in cancer, and overlap with regions of Polycomb repressive complex binding in embryonic stem cells (21–23). Notably, several dozen Polycomb targets were shared among CIMP-positive tumors from diverse origins, including breast, glioblastoma and colorectal cancers (24).

We have discovered that intrahepatic cholangiocarcinoma represents an additional human cancer with frequent mutations in *IDH1* and *IDH2*. Cholangiocarcinomas arise from the epithelial cells lining the bile duct: nearly 10% are intrahepatic, 20–25% are hepatic hilum, and 65–70% are extrahepatic (25). Mutations in a handful of candidate genes – including *KRAS*, *BRAF*, *EGFR*, *TP53*, *PIK3CA*, and *SMAD4* – have been surveyed in cholangiocarcinomas, with varying mutation frequencies in different anatomical regions of the bile duct (26). In this study, we elucidated the consequences of *IDH1* and *IDH2* mutations on DNA methylation and gene expression in intrahepatic cholangiocarcinomas and glioblastomas. We identified several genes with both increased DNA methylation and decreased gene expression that may represent candidate tumor suppressors.

Author Manuscript Author Manuscript Author Manuscript Author Manuscript

RESULTS

IDH1 and *IDH2* mutations in intrahepatic cholangiocarcinomas

We conducted whole exome sequencing of an intrahepatic cholangiocarcinoma and a non-involved liver sample from the same patient. We obtained 7.2 Gb of sequence for the tumor and 8.3 Gb for the normal liver tissues, with a mean coverage of 192x over the 44 Mb captured target regions. There were 19 predicted mutations, including an Arg132Cys mutation in the hotspot codon of *IDH1* and a Pro261Arg mutation in *RAF1*. We confirmed 8 of 19 somatic mutations (42%) as somatic by Sanger sequencing (Supplementary Table 1).

We estimated the prevalence of *IDH1* and *IDH2* mutations by sequencing exon 4 of both genes in 325 additional intrahepatic cholangiocarcinomas. We found 22 additional mutations in *IDH1* and 11 mutations in *IDH2*, for a combined frequency of 10% (Table 1). Mutation frequencies varied from 7.5% in Chinese patients (20 of 265 from Fudan University Affiliated Zhongshan Hospitals) to 25% in a predominantly Caucasian cohort (12 of 48 patients from Mayo Clinic).

Notably, 32 of 33 mutations occurred in either the hotspot codon Arg132 of *IDH1*, or the analogous codon Arg172 of *IDH2*, which mediates a conformational switch in the enzyme (27). One patient had a novel Ile99Met mutation in *IDH1*. This mutation was associated with 44% lower catalysis of isocitrate to α-KG *in vitro*, but did not gain the ability to produce 2-HG (Supplementary Figure 1). For half of the *IDH1*-mutated samples, we estimated allele frequencies using titration curves of the HT-1080 cell line as a positive control. We estimated allele frequencies between 21% and 40%, which corresponds to 42% to 80% of tumor nuclei harboring the heterozygous mutation.

Prognostic significance of *IDH1* and *IDH2* mutations in cholangiocarcinoma

In the Fudan cohort of 252 patients with follow-up data, the presence of *IDH1* or *IDH2* mutation was associated with a longer time to recurrence ($p = 0.046$) (Figure 1A). The probabilities of tumor recurrence at 1, 4 and 7 years in patients with mutated *IDH1* or *IDH2* intrahepatic cholangiocarcinomas (10.5%, 45.3% and 45.3%, respectively) were significantly lower than those with wild-type *IDH1* or *IDH2* (41.7%, 71.5% and 81.3%, respectively). The subset of patients with *IDH2* mutations had marginally longer time to recurrence ($p = 0.042$, Supplementary Figure 2). In the combined patient cohort, the presence of IDH1 or IDH2 mutation was associated with a longer overall survival ($p = 0.028$) (Figure 1B).

In univariate Cox regression analysis, *IDH1/2* mutation was significantly associated with time to recurrence (HR=0.512, 95% CI=0.273–0.960, p=0.037). Other significant clinical parameters on univariate Cox regression analysis included: tumor diameter greater than 5 cm (p=0.010); portal lymph node invasion (p=0.004); tumor without encapsulation (p=0.024) (Table 2). In multivariate analyses, the prognostic values of *IDH1/2* mutation for time to recurrence was independent of all other clinical variables tested (HR=0.477, 95% CI=0.254–0.894, p=0.021) (Table 2).

Author Manuscript Author Manuscript Author Manuscript Author Manuscript

IDH1 and *IDH2* mutations impaired the activity of α-KG-dependent TET hydroxylases and histone demethylases in intrahepatic cholangiocarcinomas

Reduction of α-KG and accumulation of 2-HG resulting from mutations in *IDH1* potentially impair the activity of multiple α-KG-dependent dioxygenases, including both the TET family of DNA dioxygenases (11), and histone lysine demethylases (11, 28). We analyzed 5hmC and 5mC by immunohistochemistry (IHC) in a panel of 36 intrahepatic cholangiocarcinomas: 19 tumors harboring a mutation in either *IDH1* or *IDH2*, and 17 tumors of similar grade but with wild-type *IDH1* and *IDH2*. Intrahepatic cholangiocarcinoma samples harboring mutant *IDH1/2* accumulated significantly lower 5hmC than those containing wild-type *IDH1/2*. The average relative intensity of 5hmC was 54.71± 8.07% in cholangiocarcinomas with wild-type *IDH1* and reduced to 24.79 ± 5.78% (p=0.005) in *IDH1*- or *IDH2*-mutated cholangiocarcinomas (Figure 2A). In contrast, cholangiocarcinomas with *IDH1* or *IDH2* mutations accumulated significantly higher 5mC than those containing wild-type *IDH1* or *IDH2*. The average relative intensity of 5mC was 21.88 ± 7.39% in cholangiocarcinomas with wild-type and increased to 60.39 ± 8.39% (p=0.002) in cholangiocarcinomas harboring a mutant *IDH1* or *IDH2* (Figure 2B). These results in cholangiocarcinomas corroborate the previous findings in gliomablastoma that mutation of *IDH1* inhibits the activity of the TET family of DNA dioxygenases, resulting in a decrease of cytosine hydroxymethylation with a concurrent increase of DNA methylation (9).

Next, we analyzed histone H3 lysine 79 (H3K79) dimethylation in the same panel of 36 cholangiocarcinoma samples. H3K79 dimethylation levels were significantly elevated in cholangiocarcinoma samples that harbor *IDH1* or *IDH2* mutation (80.79 ± 4.23%) compared to tumors with wild-type *IDH1* and *IDH2* (45.00 ± 7.11%, p = 0.0003, Figure 2C). These results indicate that mutations of *IDH1/2* genes in cholangiocarcinomas caused an inhibition of histone demethylases. In addition, we also examined the levels of HIF-1α, a transcriptional factor whose steady state level is regulated in part by the α-KG-dependent prolyl hydroxylases (PHDs). We found that tumors with *IDH1* or *IDH2* mutations also exhibited a trend towards higher levels of HIF-1α, but the significance of this increase is unclear (p = 0.151, data not shown).

IDH1 and *IDH2* mutations co-occur with *p53* inactivation in cholangiocarcinomas

The cellular effects of, and pathways affected by, mutations in *IDH1* and *IDH2* remain poorly defined. *IDH1* mutations significantly co-occur with *TP53* mutations in over 60% of low-grade astrocytomas, but the mechanism for this enrichment is unclear (29). A pathology study of multiple biopsies from the same patient has found that *IDH1* mutation occurred before the acquisition of *p53* mutation and *1p/19q* loss of heterozygosity (LOH) (30), suggesting the possibility that IDH1/2 mutation may cause a cellular stress that leads to the activation of p53 and thus increases the pressure to inactivate p53 for glioma development. We first assessed p53 expression levels by immunohistochemistry (IHC) among these cholangiocarcinomas. A tumor specimen was classified as p53-positive if immunostaining was observed in greater than 5% of tumor nuclei. Thirteen of 19 (68.4%) cholangiocarcinomas with *IDH1* or *IDH2* mutations were p53-positive, whereas only 28 of 78 (35.9%) cholangiocarcinomas without *IDH1* or *IDH2* mutations were p53-positive (p =

Author Manuscript Author Manuscript Author Manuscript Author Manuscript

0.01). In addition, the percent of tumor nuclei with p53 staining was higher among tumors with *IDH1* or *IDH2* mutations. p53 expression levels were significantly elevated in cholangiocarcinoma samples that harbor *IDH1* or *IDH2* mutation (49.63 ± 9.45%) compared to tumors with wild-type *IDH1* or *IDH2* (20.40 ± 3.98%, $p = 0.002$, Figure 2D). We next determine by direct DNA sequencing whether accumulation of p53 protein levels is associated with mutation in *p53* gene as often observed in other type of tumors. We sequenced exon 5, 6, 7, 8 and 9 that covers residues 126 to 331, which include commonly mutated hotspots. Unexpectedly, we found only one mutation in *p53* (codon 06-585) in 13 cholangiocarcinoma samples with either *IDH1* or *IDH2* mutation. In contrast, we found that p53 was mutated in 7 of 11 cholangiocarcinoma samples with with-type *IDH1* and *IDH2* (Supplementary Table 2). These results indicate that in cholangiocarcinoma, *IDH1* and *IDH2* mutation are associated with increased p53 protein levels, but not *p53* gene mutation.

IDH1 and *IDH2* mutations in cholangiocarcinomas were associated with DNA hypermethylation enriched in CpG shores

In order to localize increased DNA methylation in cholangiocarcinomas with *IDH1* or *IDH2* mutations, we surveyed over 462,000 CpG sites in CpG islands, CpG shores and intragenic regions with the Illumina HumanMethylation450 Beadchip (31). We profiled DNA methylation for 19 cholangiocarcinomas with mutations in *IDH1* or *IDH2*, as well as 31 cholangiocarcinomas without mutations in these two genes. Consensus *K*-means clustering of the 5,000 most informative CpG assays yielded two classes, with 18 of 19 *IDH1* or *IDH2* mutants segregating in one class (Fisher exact $p < 4 \times 10^{-7}$; Figure 3A). There were 7 additional cholangiocarcinomas without mutations in *IDH1* or *IDH2* that clustered with the hypermethylated samples.

We used standard *t*-tests to identify differentially methylated regions between 19 cholangiocarcinomas with mutations in *IDH1* or *IDH2*, compared with 31 cholangiocarcinomas without mutations in these genes. We identified 5,763 CpG sites at a Benjamini-Hochberg False Discovery Rate of 1% and a change in methylation beta-value greater than 0.20. Hypermethylation was predominant: 5,758 CpG sites associated with 2,309 genes had significantly increased methylation, while only 5 CpG sites associated with 4 genes had significantly decreased methylation (Figure 3B; Supplementary Table 3).

The context of CpG sites relative to annotated transcripts allows us to infer how methylation may affect the regulation of gene expression. We observed a 1.6-fold enrichment of differentially methylated CpG sites within CpG shores in cholangiocarcinomas (Fisher exact $p < 10^{-16}$) (Figure 3C). Genomic regions between 200 bp and 1500 bp upstream of transcription start sites were 1.75-fold enriched for increased CpG methylation (Fisher exact $p < 10^{-16}$) (Figure 3D). In contrast, intragenic methylation was 0.67-fold less susceptible for DNA hypermethylation (Fisher exact $p < 10^{-16}$). Taken together, these annotations suggest that hypermethylated CpG sites in cholangiocarcinomas may modulate gene expression. Gene Set Enrichment Analysis of hypermethylated target genes yielded 3 gene sets, including regulation of actin cytoskeleton, axon guidance and inositol 1,4,5-triphosphate signaling (Supplementary Figure 3A; Supplementary Table 4).

Author Manuscript Author Manuscript Author Manuscript Author Manuscript

Gene expression changes associated with mutations in *IDH1* or *IDH2* in cholangiocarcinomas

One consequence of DNA methylation upstream of genes can be the silencing of gene expression. We compared global gene expression profiles between 7 cholangiocarcinomas with *IDH1* or *IDH2* mutations and 20 tumors without these mutations (32). Among the 2,309 genes with increased methylation in tumors with *IDH1* or *IDH2* mutations, 29 genes had a ≥3-fold increase in gene expression and 99 genes had ≥3-fold reduction in gene expression (Figure 4A). Genes with both elevated DNA methylation and reduced gene expression could represent potential direct targets of *IDH1* and *IDH2* mutations. Ingenuity Pathway Analysis on these 128 genes revealed a signaling network that included cytokine and NF-κB signaling (Figure 4B).

We used Gene Set Enrichment Analysis to compare the global gene expression profiles of the *IDH1/2* mutant and *IDH1/2*-wild-type cholangiocarcinomas. The small number of samples reduced the significance of these findings, yet there were some intriguing trends. Notably, 4 overlapping gene sets implicated upregulation of the *FGFR* signaling pathway, and the *FGFR2*, *FGFR3* and *FGFR4* receptor tyrosine kinases were overexpressed at least 3-fold among tumors with *IDH1* or *IDH2* mutations (FDR q-value = 0.054; Fig. 4C to 4E). Carboxylic acid transporters, epigenetic regulators and cell proliferation gene sets were downregulated among the cholangiocarcinomas with *IDH1* or *IDH2* mutations (Supplementary Figure 4). Other upregulated gene sets included proteoglycan and heparin sulfate metabolism, protein folding, membrane fusion, transcription from RNA polymerase III. (GSEA nominal p-value < 0.05; FDR q-value = 1, Supplementary Figure 4).

Differentially methylated regions in *IDH1*-mutated glioblastomas

We sought to assess whether *IDH1* mutations instigate DNA methylation of similar genomic regions, when the mutations occur in the context of different tissue types. We profiled DNA methylation of 26 glioblastomas with *IDH1* mutations, as well as 36 glioblastomas without mutations. We identified 47,291 hypermethylated CpG sites among 9,394 genes that were associated with *IDH1* mutations, at a False Discovery Rate of 1% and a change in methylation beta-value greater than 0.20. These 62 samples were representative of the 91 glioblastomas in The Cancer Genome Atlas cohort (15) (Supplementary Figure 5).

Methylated targets in glioblastomas were enriched for genes involved in neuronal biology. Gene set enrichment analysis yielded 97 gene sets that merged into 11 annotation clusters of overlapping gene sets (FDR q < 0.01; Supplementary Figure 3B, Supplementary Table 5). Methylated gene targets were enriched in neuronal biology, including neuronal differentiation, synaptic transmission, ion transport, insulin secretion, NF-kappaB signaling, cAMP signaling, axon guidance, regulation of actin cytoskeleton, calmodulin pathway, MAPK pathways, G protein signaling, and Rho GTPases. Assuming that methylation is associated with gene silencing, these annotations suggest that *IDH1*-mediated DNA hypermethylation counteracts neuronal differentiation in glioblastomas, and provides further evidence for the model that *IDH1* mutations may occur in a neural progenitor cell of origin.

Author Manuscript Author Manuscript Author Manuscript Author Manuscript

Commonly hypermethylated regions in cholangiocarcinomas and glioblastomas with mutations in *IDH1* or *IDH2*

We identified the overlap of hypermethylated CpG sites in cholangiocarcinomas or glioblastomas with mutations in *IDH1* or *IDH2*, compared to the same tumor types without mutations. Nearly half of the hypermethylated genes in cholangiocarcinomas were also methylated in glioblastomas: 2,681 hypermethylated CpG sites with a methylation beta-value difference greater than 0.20 that were adjacent to 1,149 genes, which represented a nearly 10-fold enrichment compared with random chance (Figure 5A; χ^2 test $p < 10^{-15}$). We integrated the list of hypermethylated genes from methylation arrays with two external gene expression datasets with known *IDH1* mutation status: a set of 71 proneural glioblastomas (15) and a set of 27 cholangiocarcinomas (32). We hypothesized that *IDH1* or *IDH2* mutations would have similar effects on methylation and gene expression across different patient cohorts. We filtered for genes with increased DNA methylation and lower gene expression in both tumor types. Among the 867 genes that were represented on both microarray platforms, we found 129 genes (15%) with at least two-fold decrease in gene expression among cholangiocarcinomas with *IDH1* or *IDH2* mutations, and 43 genes (5%) with at least 2-fold decrease among glioblastomas with *IDH1* mutations. Sixteen hypermethylated genes had reduced gene expression in both tumor types: *RBP1*, *MT1M*, *FMOD*, *LOX*, *RAB34*, *ENPP2*, *RGS16*, *KCTD14*, *MDK*, *S100A9*, *PRKCDBP*, *SPAG17*, *FHL2*, *C11orf45*, *LRRC34* and *TSHZ2* (Figure 5B, Supplementary Table 6).

DISCUSSION

We have discovered intrahepatic cholangiocarcinomas as an additional and fifth major tumor type with frequent mutations (~9%) in *IDH1* and *IDH2*. These mutations occurred predominantly in hotspot codons, *IDH1* Arg132 and *IDH2* Arg172, and were associated with decreased 5-hydroxymethylcytosine, increased DNA methylation, increased H3K79 dimethylation, and increased p53 expression. The prognostic significance of mutations in *IDH1* and *IDH2* suggests that hypermethylated cholangiocarcinomas may represent a distinct molecular sub-class with a better prognosis.

Recently, Borger et al. have carried out a genotyping study of 287 tumor samples including multiple kinds of gastrointestinal cancer, targeting *IDH1* Arg132 or *IDH2* Arg172, but not *IDH2* Arg140, which is a mutation hotpot in AML (33). They identified *IDH1/2* mutations in 9 of 40 (23%) intrahepatic cholangiocarcinoma, but none in 22 extrahepatic cholangiocarcinoma or 25 gallbladder carcinoma (34). In that study, mutations in *IDH1* had higher prevalence than mutations in *IDH2* (8 out of 9, or 89%), and both mutations were associated with higher levels of 2-hydroxyglutarate. More recently, Kipp et al found *IDH1/2* mutations in 21 of 94 cholangiocarcinomas, including 19 of 67 intrahepatic cholangiocarcinomas (35). Tumors with *IDH1/2* mutations were poorly differentiated with clear cell change. Together with this current report, these three studies identified 62 of 433 (14%) intrahepatic cholangiocarcinomas with mutation in either *IDH1* or *IDH2*. There appears to be clear difference in the frequency of *IDH1/2* mutation prevalence, which appears to be lower in Asian patients (7.5%), compared with 23% in the Borger et al cohort, 28% of intrahepatic tumors in the Kipp et al cohort, as well as in 25% (12 of 48) of patients

Author Manuscript Author Manuscript Author Manuscript Author Manuscript

in this current cohort from Mayo Clinic. Both the molecular basis and clinical significance of this ethnic difference in *IDH1/2* mutations remain to be determined.

The earliest genetic alterations during the development of secondary GBM are mutations targeting *IDH1* and *p53* with *IDH1* mutations likely occurring before *p53* mutation (29, 30). This association suggests that *IDH1/2* mutation may cause a cellular stress that leads to the activation of p53 and thus increases the pressure to inactivate p53 for glioma development. Our study showed that mutations in *IDH1* or *IDH2* likely also cause a cellular stress in cholangiocarcinomas that leads to p53 activation, as seen by the significant increase of p53 protein levels. Unlike secondary GBM, mutations in *IDH1* or *IDH2* in cholangiocarcinomas are not associated with *p53* gene mutation. We interpret our result as an indication that unlike GBM, an alteration of a gene downstream p53 pathway, rather than p53 gene itself, may occur in cholangiocarcinomas with *IDH1* or *IDH2* mutation that has functionally inactivated the p53 pathway and relived the pressure to mutate *p53*.

A common theme among diverse tumors with mutations in the *IDH-TET* pathway may be the expansion of progenitor lineages, as a consequence of widespread disruptions in DNA methylation and hydroxymethylation. The impairment of hematopoetic stem cell differentiation can be facilitated by *IDH2* mutations or reduced Tet2 (10, 36). Glioblastomas with *IDH1* mutations are strongly associated with the expression of marker genes from neuroblast progenitors (16), and our data indicate that concomitant methylation of neuronal differentiation genes occurs in glioblastomas with *IDH1* mutations. Mutations in the *IDH-TET* pathway may appear early in tumor progression: *IDH1* or *TET2* mutations occur at high frequencies in low grade gliomas or myeloproliferative neoplasms, respectively, while subsequent mutations in *TP53* or *JAK2* coincide with the transition to myeloid leukemias or glioblastomas (30, 37). We speculate that the precursor lineages for hepatocytes and cholangiocytes that reside in bile ducts may be expanded in cholangiocarcinomas with mutations in *IDH1* or *IDH2* (38). Tumors with *IDH1/2* mutations expressed over 1.6-fold higher levels of the hepatic stem cell lineage markers, EpCAM and NCAM (Supplementary Figure 6) (39). This model that invokes a precursor cell of origin within the liver may explain why lower frequencies of *IDH1* or *IDH2* mutations were observed in extrahepatic cholangiocarcinomas (34, 35).

Genome-wide surveys of CpG island methylation indicated that there was significant overlap of DNA hypermethylation between two tumor types with *IDH1* mutations. These overlapping hypermethylated regions may include tumor suppressors that are silenced in multiple cancer types. Divergent target genes in different tumor types may reflect differences in chromatin modifications or accessibility to TET dioxygenases between distinct mature cell lineages. In multiple studies of DNA methylation and gene expression, only a minority of genes have reduced gene expression: for instance, 17% of genes in CIMP-high gliomas (15), 7% of genes in CIMP-high colorectal cancer (40), and 6% of genes in CIMP-high breast cancers (24). This modest impact may be due to several reasons. Methylation in different regions relative to the transcription start site have different efficacies in inhibiting transcription (41). Genes that accumulate methylation may have low baseline expression in most tumors, and thus an increase in DNA methylation may not silence expression levels further (15). In addition, the impact of DNA methylation on

Author Manuscript Author Manuscript Author Manuscript Author Manuscript

noncoding transcripts could not be assayed by gene expression microarrays. Further integration of DNA hypermethylated regions with gene expression data will help to identify the target genes whose expression are affected by the mutations in *IDH1/2* as the result of altered histone or DNA methylation.

MATERIALS & METHODS

Tumor biospecimens

Snap frozen or paraffin-embedded tumor and non-tumor specimens were procured after obtaining written informed consent under Institutional Review Board guidelines from 319 patients with intrahepatic cholangiocarcinoma who received surgical treatments at Liver Cancer Institute and Zhongshan Hospital of Fudan University (Shanghai, China) (265 cases), the University of North Carolina (13 cases), and Mayo Clinic (48 cases). Tumors were verified as cholangiocarcinoma by two pathologists. The 252 out of 265 cholangiocarcinoma patients from Fudan University were enrolled into the survival analysis, they were followed up to May 15, 2011, with a median follow-up of 11.00 months (range 1–110.13 months). The 41 of 48 patients from Mayo Clinic were also enrolled into the survival analysis, with a median follow-up of 29.53 months (range 0.67–153.43 months).

Glioblastoma biospeciments – including 26 tumors with *IDH1* mutations and 36 tumors without *IDH1* mutations – were acquired from Affiliated Huashan Hospital of Fudan University. A physician or nurse practitioner obtained informed consent from the patients. The procedures related to human subjects were approved by Ethic Committee of the Institutes of Biomedical Sciences (IBS), Fudan University.

Whole exome sequencing

Three micrograms of genomic DNA from an intrahepatic cholangiocarcinoma – as well as adjacent, non-involved liver tissue – were fragmented using Bioruptor sonication device (Diagenode), Illumina paired end adapters were ligated, and enriched by 6 cycles of PCR amplification. Whole exome capture was performed with SureSelect Human All Exon kit (Agilent) using 500 ng of amplified library, hybridized DNA fragments were captured with streptavidin-coated beads, and amplified by 12 cycles of PCR. Paired-end 76 bp sequence reads were generated on the Genome Analyzer II and HiSeq 2000 sequencers (Illumina). Somatic mutations were called by the MuTect algorithm (42) and validated by PCR using primers in Supplementary Table 1.

DNA sequencing

DNA was extracted using the QIAamp DNA mini kit for snap frozen samples, or the Qiagen DNA FFPE tissue kit for paraffin-embedded samples. Exon 4 of *IDH1* was PCR amplified using the primer pair *IDH1*-f: TGAGCTCTATATGCCATCACTGCA and *IDH1*-r: CAATTTCATACCTTGCTTAATGGG for 30 cycles with the following conditions: 94°C for 30s, 55°C for 30s, 72°C for 30s. Exon 4 of *IDH2* was similarly PCR amplified with the primer pair IDH2-f: GTCTGGCTGTGTTGTTGCTTG and IDH2-r: CAGAGACAAGAGGATGGCTAGG. DNA samples from paraffin sections were subjected to a second round of PCR using the nested primers: IDH1-NestF:

Author Manuscript Author Manuscript Author Manuscript Author Manuscript

GCAGTTGTAGGTTATAACTATCC and IDH1-NestR: TGGGTGTAGATACCAAAAG, or IDH2-NestF: GGGTTCAAATTCTGGTTGAAAG and IDH2-NestR: GGCGAGGAGCTCCAGTCG. Pyrosequencing confirmation of *IDH1* and *IDH2* mutations was performed using the primers in (4).

Sequencing of exon 5–9 of the *TP53* gene was carried out following the method from IARC TP53 database (http://www-p53.iarc.fr/Download/TP53_DirectSequencing_IARC.pdf) with following primers: Exon 5-6-f: TGTTCACTTGTGCCCTGACT and Exon 5-6-r: TTAACCCCTCCTCCCAGAGA; Exon 7-f: AGGCACACTGGCCTCATCTT and Exon 7-r: TGTGCAGGGTGGCAAGTGGC; Exon 8-9-f: TTGGGAGTAGATGGAGCCT and Exon 8-9-r: AGTGTTAGACTGGAAACTTT.

Statistical analysis of clinical and pathological data

Analysis was performed with SPSS 16.0 for Windows (SPSS, Chicago, IL, USA). The endpoint was the time to recurrence (TTR) and overall survival (OS). TTR was defined as the time from the start of surgery to the first report of intrahepatic recurrence (excluding patients who had died from non-liver cancer causes before recurrence). For patients who had not experienced a recurrence at the time of death or last follow-up, TTR was censored at the date of death or the last follow-up. A diagnosis of recurrence was based on typical imaging appearance in CT and/or MRI scan. OS was defined as the interval between the dates of surgery and death (43). TTR and OS were compared with the Kaplan-Meier method, and the significance was determined by the log-rank test. The Cox regression model was applied to evaluate the effect of each clinical variable and the mutation type on TTR. Hazard ratios (HRs) for the significant mutation were calculated with adjustments for clinicopathologic characteristics.

Immunohistochemistry

Tissue sections were deparaffinized twice by xylene and then hydrated. Hydrogen peroxide (0.6%) was used to eliminate endogenous peroxidase activity. The sections were blocked with goat serum in Tris-buffered saline for 30 min. Sections were then incubated with anti-5-methylcytosine antibody (1:50; Calbiochem), anti-5-hydroxymethylcytosine antibody (1:2500; Active Motif), anti-H3K79me2 antibody (1:500; Abcam), or anti-p53 antibody (1:300; Leica) overnight at 4°C. Secondary antibody was then applied and incubated at 37°C for 1 hour. Sections were developed with diaminobenzidine and stopped with water. To quantify the positively stained areas in samples, five fields from each sample were randomly selected and microscopically examined by an expert pathologist and a scientist without knowledge of other characteristics of the samples. The density of positive staining was evaluated using a Leica CCD camera DFC420 connected to a Leica DMIRE2 microscope (Leica Microsystems Imaging Solutions, Cambridge, UK). Photographs of representative fields were captured by the Leica QWin Plus v3 software. The average positive area was calculated by dividing the positively stained areas over total area.

HumanMethylation450 BeadChip assays

The Zymo EZ DNA Methlyation kit was used for bisulfite treatment of 500 ng of genomic DNA. Bisulfite-converted DNA was hybridized to the Illumina HumanMethylation450

Author Manuscript Author Manuscript Author Manuscript Author Manuscript

BeadChips according to the manufacturer's instructions, and normalized beta values after background correction were reported by Illumina GenomeStudio software. Data were deposited in the NCBI Gene Expression Omnibus (http://www.ncbi.nlm.nih.gov/geo/), accession number GSE32286.

Identification of differentially methylated CpG sites

We filtered out CpG sites for which the average methylation beta-value was less than 0.70 from 4 technical replicates of genomic DNA from a *M.SssI*-treated methylated control. Probes on chromosomes X and Y were discarded, which left 462,732 CpG assays. Thirty tumors were assayed at Wake Forest Baptist Medical Center, and twenty tumors were assays that the University of North Carolina. We modeled the logit-transformed beta values for each CpG assay with a sample-size-weighted linear model to adjust for the batch effect:

$$logit\,(\beta_i)=\alpha Batch+\gamma Mutant+\varepsilon_i$$

where *Batch* is an indicator variable for the batch effect taking value 1 if it was processed at the University of North Carolina, and *Mutant* is an indicator variable for the mutation status of *IDH1* or *IDH2* taking value 1 if it was mutant. The estimated batch effect α was subtracted from the logit transformed beta values in Batch 2, and back-transformed to obtain the normalized beta values. After the normalization step, probes that were differentially methylated between *IDH1/2*-mutant and wildtype tumors were obtained using the standard two-sample *t*-test with unequal variance and sample size. To adjust for multiple comparisons, we applied the Benjamini-Hochberg method to control the False Discovery Rate at 5%. We further filtered the list of significant CpGs by retaining those which exhibited at least 20% difference in methylation beta-value between mutant and wildtype in our final comparisons.

Consensus clustering

We determined the top 5,000 CpG probes with the highest median absolute deviation across the 50 cholangiocarcinoma samples. We used the R clusterCons package to perform *K*-means clustering for values ranging from *K*=2 to *K*=5, with 500 iterations of randomly resampling 80% of the probes and 80% of the tumors. We chose *K*=2 as the best performing cluster.

Gene expression microarrays

Microarray data for 27 fresh-frozen intrahepatic cholangiocarcinomas were obtained from the NCBI Gene Expression Omnibus (http://www.ncbi.nlm.nih.gov/geo/), accession number GSE26566 (32). Data preprocessing was performed with GenomeStudio v2010 as described in (44). Intensity values less than 1 was transformed to 1, and the data set quantile normalized. Tumor samples were analyzed as the log2 ratio to the average of 6 normal intrahepatic bile ducts that were resected at the Surgical Branch of the National Institutes of Health. There were 15,504 genes with significant detection p-values ($p < 0.05$) and median absolute deviation greater than 0 across 27 tumors.

Author Manuscript Author Manuscript Author Manuscript Author Manuscript

Copy-number normalized gene expression changes between CpG Island Methylator Phenotype positive and negative proneural glioblastomas was contained in a table of 1520 hypermethylated genes from the Supplementary Information of (15).

Gene set enrichment analysis of methylated CpG sites

For each CpG assay, a *t* statistic was calculated between the logit-transformed beta values for 19 *IDH1* or *IDH2* mutated cholangiocarcinomas, versus 31 *IDH1* and *IDH2* wildtype cholangiocarcinomas. Similarly, the *t* statistic was calculated between 26 *IDH1*-mutated glioblastomas versus 36 *IDH1*-wildtype glioblastomas. Gene scores were assigned as the maximum *t*-statistic for all CpG assays annotated to a particular gene. In the combined analysis of cholangiocarcinomas and glioblastomas, a gene score was assigned as the maximum coefficient for the mutant-associated coefficient (Supplementary Methods). Gene set enrichment analysis version 2.07 was run in pre-ranked mode on a list of 19,728 genes covered in the HumanMethylation450 BeadChip after probe filtering (45). A total of 1,284 gene sets were obtained from merging Gene Ontology biological process terms with the mSigDB version 3.0 signaling pathways curated from KEGG, BioCarta and Reactome. Annotation enrichments were visualized with the Enrichment Map plugin for Cytoscape (46), using a nominal *p*-value cutoff of 0.001, a FDR *q*-value cutoff of 0.10 (cholangiocarcinomas) or 0.01 (glioblastomas), and an overlap of 50% between gene sets.

Signaling pathway annotations of gene expression data

Gene Set Enrichment Analysis version 2.07 was run on the list of 15,504 genes covered in the Illumina HumanRef-8v2 BeadChips after filtering (45). A total of 1,284 gene sets were obtained from merging Gene Ontology biological process terms with the mSigDB version 3.0 signaling pathways curated from KEGG, BioCarta and Reactome. Ingenuity Pathway Analysis annotated the list of 285 genes in intrahepatic cholangiocarcinoma with significant DNA hypermethylation as well as >2.8-fold reduction in gene expression, in *IDH1/2*-mutated versus *IDH1/2*-wildtype tumors.

Supplementary Material

Refer to Web version on PubMed Central for supplementary material.

Acknowledgments

The UNC Biospecimen Core Facility, Mammalian Genotyping Core Facility and Translational Pathology Laboratory provided technical assistance for this study. Funding for this research was provided by: the 985 Program from the Chinese Ministry of Education [K.L.G., Y.X.], MOST 973 (No. 2009CB918401, No. 2011CB910600, No. 2012CB910300, No. 2012CB910101) [D.Y., Y.X. and K.L.G.]; The NSFC Program of International Cooperation and Exchanges (No. 81120108016) [L.X.Q., Y. X] and China National Key Projects for Infectious Disease (2008ZX10002-021, 2012ZX10002-012) [L.Z.Q.], National Institutes of Health [K.L.G., Y.X., S.S.T., L.R.R.], James S. McDonnell Foundation [Y.X.], Samuel Waxman Cancer Research Foundation [Y.X.], American Gastroenterological Association Foundation for Digestive Health and Nutrition [L.R.R.], Alfred P. Sloan Foundation fellowship [D.Y.C.], Nancy Stegman Cancer Research Fund [D.Y.C.], University Cancer Research Fund [D.Y.C., Y.X.].

Author Manuscript Author Manuscript Author Manuscript Author Manuscript

References

1. Yan H, Parsons DW, Jin GL, McLendon R, Rasheed BA, Yuan WS, et al. IDH1 and IDH2 Mutations in Gliomas. N Engl J Med. 2009; 360:765–73. [PubMed: 19228619]
2. Marcucci G, Maharry K, Wu YZ, Radmacher MD, Mrozek K, Margeson D, et al. IDH1 and IDH2 gene mutations identify novel molecular subsets within de novo cytogenetically normal acute myeloid leukemia: A Cancer and Leukemia Group B Study. J Clin Oncol. 2010; 28:2348–55. [PubMed: 20368543]
3. Amary MF, Bacsi K, Maggiani F, Damato S, Halai D, Berisha F, et al. IDH1 and IDH2 mutations are frequent events in central chondrosarcoma and central and periosteal chondromas but not in other mesenchymal tumours. J Pathol. 2011; 224:334–43. [PubMed: 21598255]
4. Shibata T, Kokubu A, Miyamoto M, Sasajima Y, Yamazaki N. Mutant IDH1 confers an in vivo growth in a melanoma cell line with BRAF mutation. Am J Pathol. 2011; 178:1395–402. [PubMed: 21356389]
5. Amary MF, Damato S, Halai D, Eskandarpour M, Berisha F, Bonar F, et al. Ollier disease and Maffucci syndrome are caused by somatic mosaic mutations of IDH1 and IDH2. Nat Genet. 2011; 43:1262–5. [PubMed: 22057236]
6. Pansuriya TC, van Eijk R, d'Adamo P, van Ruler MA, Kuijjer ML, Oosting J, et al. Somatic mosaic IDH1 and IDH2 mutations are associated with enchondroma and spindle cell hemangioma in Ollier disease and Maffucci syndrome. Nat Genet. 2011; 43:1256–61. [PubMed: 22057234]
7. Zhao SM, Lin Y, Xu W, Jiang WQ, Zha ZY, Wang P, et al. Glioma-derived mutations in IDH1 dominantly inhibit IDH1 catalytic Activity and induce HIF-1 alpha. Science. 2009; 324:261–5. [PubMed: 19359588]
8. Dang L, White DW, Gross S, Bennett BD, Bittinger MA, Driggers EM, et al. Cancer-associated IDH1 mutations produce 2-hydroxyglutarate. Nature. 2009; 462:739–U52. [PubMed: 19935646]
9. Xu W, Yang H, Liu Y, Yang Y, Wang P, Kim SH, et al. Oncometabolite 2-hydroxyglutarate is a competitive inhibitor of alpha-ketoglutarate-dependent dioxygenases. Cancer Cell. 2011; 19:17–30. [PubMed: 21251613]
10. Figueroa ME, Abdel-Wahab O, Lu C, Ward PS, Patel J, Shih A, et al. Leukemic IDH1 and IDH2 mutations result in a hypermethylation phenotype, disrupt TET2 function, and impair hematopoeitic differentiation. Cancer Cell. 2010; 18:553–67. [PubMed: 21130701]
11. Tahiliani M, Koh KP, Shen Y, Pastor WA, Bandukwala H, Brudno Y, et al. Conversion of 5-methylcytosine to 5-hydroxymethylcytosine in mammalian DNA by MLL partner TET1. Science. 2009; 324:930–5. [PubMed: 19372391]
12. Ito S, D'Alessio AC, Taranova OV, Hong K, Sowers LC, Zhang Y. Role of Tet proteins in 5mC to 5hmC conversion, ES-cell self-renewal and inner cell mass specification. Nature. 2010; 466:1129–33. [PubMed: 20639862]
13. Ito S, Shen L, Dai Q, Wu SC, Collins LB, Swenberg JA, et al. Tet proteins can convert 5-methylcytosine to 5-formylcytosine and 5-carboxylcytosine. Science. 2011; 333:1300–3. [PubMed: 21778364]
14. He YF, Li BZ, Li Z, Liu P, Wang Y, Tang Q, et al. Tet-mediated formation of 5-carboxylcytosine and its excision by TDG in mammalian DNA. Science. 2011; 333:1303–7. [PubMed: 21817016]
15. Noushmehr H, Weisenberger DJ, Diefes K, Phillips HS, Pujara K, Berman BP, et al. Identification of a CpG Island Methylator Phenotype that Defines a Distinct Subgroup of Glioma. Cancer Cell. 2010; 17:510–22. [PubMed: 20399149]
16. Verhaak RGW, Hoadley KA, Purdom E, Wang V, Qi Y, Wilkerson MD, et al. Integrated genomic analysis identifies clinically relevant subtypes of glioblastoma characterized by abnormalities in PDGFRA, IDH1, EGFR, and NF1. Cancer Cell. 2009; 17:98–110. [PubMed: 20129251]
17. Parsons DW, Jones S, Zhang X, Lin JC, Leary RJ, Angenendt P, et al. An integrated genomic analysis of human glioblastoma multiforme. Science. 2008; 321:1807–12. [PubMed: 18772396]
18. Toyota M, Ahuja N, Ohe-Toyota M, Herman JG, Baylin SB, Issa JP. CpG island methylator phenotype in colorectal cancer. Proc Natl Acad Sci U S A. 1999; 96:8681–6. [PubMed: 10411935]

Author Manuscript Author Manuscript Author Manuscript Author Manuscript

19. Nagasaka T, Sasamoto H, Notohara K, Cullings HM, Takeda M, Kimura K, et al. Colorectal cancer with mutation in BRAF, KRAS, and wild-type with respect to both oncogenes showing different patterns of DNA methylation. J Clin Oncol. 2004; 22:4584–94. [PubMed: 15542810]
20. Jones PA, Baylin SB. The epigenomics of cancer. Cell. 2007; 128:683–92. [PubMed: 17320506]
21. Widschwendter M, Fiegl H, Egle D, Mueller-Holzner E, Spizzo G, Marth C, et al. Epigenetic stem cell signature in cancer. Nature Genet. 2007; 39:157–8. [PubMed: 17200673]
22. Ohm JE, McGarvey KM, Yu X, Cheng LZ, Schuebel KE, Cope L, et al. A stem cell-like chromatin pattern may predispose tumor suppressor genes to DNA hypermethylation and heritable silencing. Nat Genet. 2007; 39:237–42. [PubMed: 17211412]
23. Schlesinger Y, Straussman R, Keshet I, Farkash S, Hecht M, Zimmerman J, et al. Polycomb-mediated methylation on Lys27 of histone H3 pre-marks genes for de novo methylation in cancer. Nat Genet. 2007; 39:232–6. [PubMed: 17200670]
24. Fang F, Turcan S, Rimner A, Kaufman A, Giri D, Morris LG, et al. Breast cancer methylomes establish an epigenomic foundation for metastasis. Sci Transl Med. 2011; 3:75ra25.
25. Blechacz B, Gores GJ. Cholangiocarcinoma: Advances in pathogenesis, diagnosis, and treatment. Hepatology. 2008; 48:308–21. [PubMed: 18536057]
26. Hezel AF, Deshpande V, Zhu AX. Genetics of biliary tract cancers and emerging targeted therapies. J Clin Oncol. 2010; 28:3531–40. [PubMed: 20547994]
27. Yang B, Zhong C, Peng YJ, Lai Z, Ding JP. Molecular mechanisms of “off-on switch” of activities of human IDH1 by tumor-associated mutation R132H. Cell Res. 2010; 20:1188–200. [PubMed: 20975740]
28. Xu Y, Wu F, Tan L, Kong L, Xiong L, Deng J, et al. Genome-wide regulation of 5hmC, 5mC, and gene expression by Tet1 hydroxylase in mouse embryonic stem cells. Mol Cell. 2011; 42:451–64. [PubMed: 21514197]
29. Dunn GP, Rinne ML, Wykosky J, Genovese G, Quayle SN, Dunn IF, et al. Emerging insights into the molecular and cellular basis of glioblastoma. Genes Dev. 2012; 26:756–84. [PubMed: 22508724]
30. Watanabe T, Nobusawa S, Kleihues P, Ohgaki H. IDH1 mutations are early events in the development of astrocytomas and oligodendrogliomas. Am J Pathol. 2009; 174:1149–53. [PubMed: 19246647]
31. Aishima S, Kuroda Y, Nishihara Y, Taguchi K, Taketomi A, Maehara Y, et al. Gastric mucin phenotype defines tumour progression and prognosis of intrahepatic cholangiocarcinoma: gastric foveolar type is associated with aggressive tumour behaviour. Histopathology. 2006; 49:35–44. [PubMed: 16842244]
32. Andersen JB, Spee B, Bechacz BR, Avital I, Komuta M, Barbour A, et al. Genomic and genetic characterization of cholangiocarcinoma identifies therapeutic targets for tyrosine kinase inhibitors. Gastroenterology. 2012; 142:1021–31. [PubMed: 22178589]
33. Ward PS, Patel J, Wise DR, Abdel-Wahab O, Bennett BD, Coller HA, et al. The Common Feature of Leukemia-Associated IDH1 and IDH2 Mutations Is a Neomorphic Enzyme Activity Converting alpha-Ketoglutarate to 2-Hydroxyglutarate. Cancer Cell. 2010; 17:225–34. [PubMed: 20171147]
34. Borger DR, Tanabe KK, Fan KC, Lopez HU, Fantin VR, Straley KS, et al. Frequent mutation of Isocitrate Dehydrogenase (IDH)1 and IDH2 in cholangiocarcinoma identified through broad-based tumor genotyping. Oncologist. in press.
35. Kipp BR, Voss JS, Kerr SE, Barr Fritcher EG, Graham RP, Zhang L, et al. Isocitrate dehydrogenase 1 and 2 mutations in cholangiocarcinoma. Hum Pathol. 2012
36. Moran-Crusio K, Reavie L, Shih A, Abdel-Wahab O, Ndiaye-Lobry D, Lobry C, et al. Tet2 loss leads to increased hematopoietic stem cell self-renewal and myeloid transformation. Cancer Cell. 2011; 20:11–24. [PubMed: 21723200]
37. Abdel-Wahab O, Manshouri T, Patel J, Harris K, Yao JJ, Hedvat C, et al. Genetic analysis of transforming events that convert chronic myeloproliferative neoplasms to leukemias. Cancer Res. 2010; 70:447–52. [PubMed: 20068184]
38. Turner R, Lozoya O, Wang Y, Cardinale V, Gaudio E, Alpini G, et al. Human hepatic stem cell and maturational liver lineage biology. Hepatology. 2011; 53:1035–45. [PubMed: 21374667]

Author Manuscript Author Manuscript Author Manuscript Author Manuscript

39. Cardinale V, Wang Y, Carpino G, Mendel G, Alpini G, Gaudio E, et al. The biliary tree-a reservoir of multipotent stem cells. Nat Rev Gastroenterol Hepatol. 2012; 9:231–40. [PubMed: 22371217]
40. Hinoue T, Weisenberger DJ, Lange CP, Shen H, Byun HM, Van Den Berg D, et al. Genome-scale analysis of aberrant DNA methylation in colorectal cancer. Genome Res. 2012; 22:271–82. [PubMed: 21659424]
41. Brenet F, Moh M, Funk P, Feierstein E, Viale AJ, Socci ND, et al. DNA methylation of the first exon is tightly linked to transcriptional silencing. PLoS One. 2011; 6:e14524. [PubMed: 21267076]
42. Chapman MA, Lawrence MS, Keats JJ, Cibulskis K, Sougnez C, Schinzel AC, et al. Initial genome sequencing and analysis of multiple myeloma. Nature. 2011; 471:467–72. [PubMed: 21430775]
43. Llovet JM, Di Bisceglie AM, Bruix J, Kramer BS, Lencioni R, Zhu AX, et al. Design and endpoints of clinical trials in hepatocellular carcinoma. J Natl Cancer Inst. 2008; 100:698–711. [PubMed: 18477802]
44. Andersen JB, Factor VM, Marquardt JU, Raggi C, Lee YH, Seo D, et al. An integrated genomic and epigenomic approach predicts therapeutic response to zebularine in human liver cancer. Sci Transl Med. 2010; 2:54ra77.
45. Subramanian A, Tamayo P, Mootha VK, Mukherjee S, Ebert BL, Gillette MA, et al. Gene set enrichment analysis: a knowledge-based approach for interpreting genome-wide expression profiles. Proc Natl Acad Sci U S A. 2005; 102:15545–50. [PubMed: 16199517]
46. Merico D, Isserlin R, Stueker O, Emili A, Bader GD. Enrichment map: a network-based method for gene-set enrichment visualization and interpretation. PLoS One. 2010; 5:e13984. [PubMed: 21085593]

Author Manuscript Author Manuscript Author Manuscript Author Manuscript

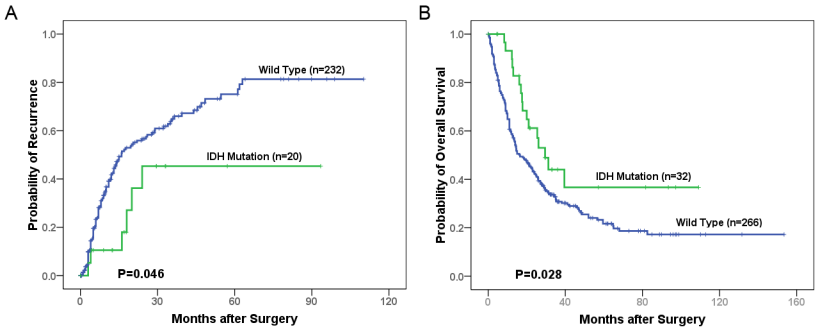

Figure 1. *IDH1/2* mutations were associated with better prognosis in intrahepatic cholangiocarcinoma

Inverse Kaplan-Meier curves plot the (A) time to recurrence after surgical resection in a cohort of 252 intrahepatic cholangiocarcinoma patients, or (B) overall survival in a combined cohort of 298 intrahepatic cholangiocarcinomas patients. The significance was determined by the log-rank test.

Author Manuscript Author Manuscript Author Manuscript Author Manuscript

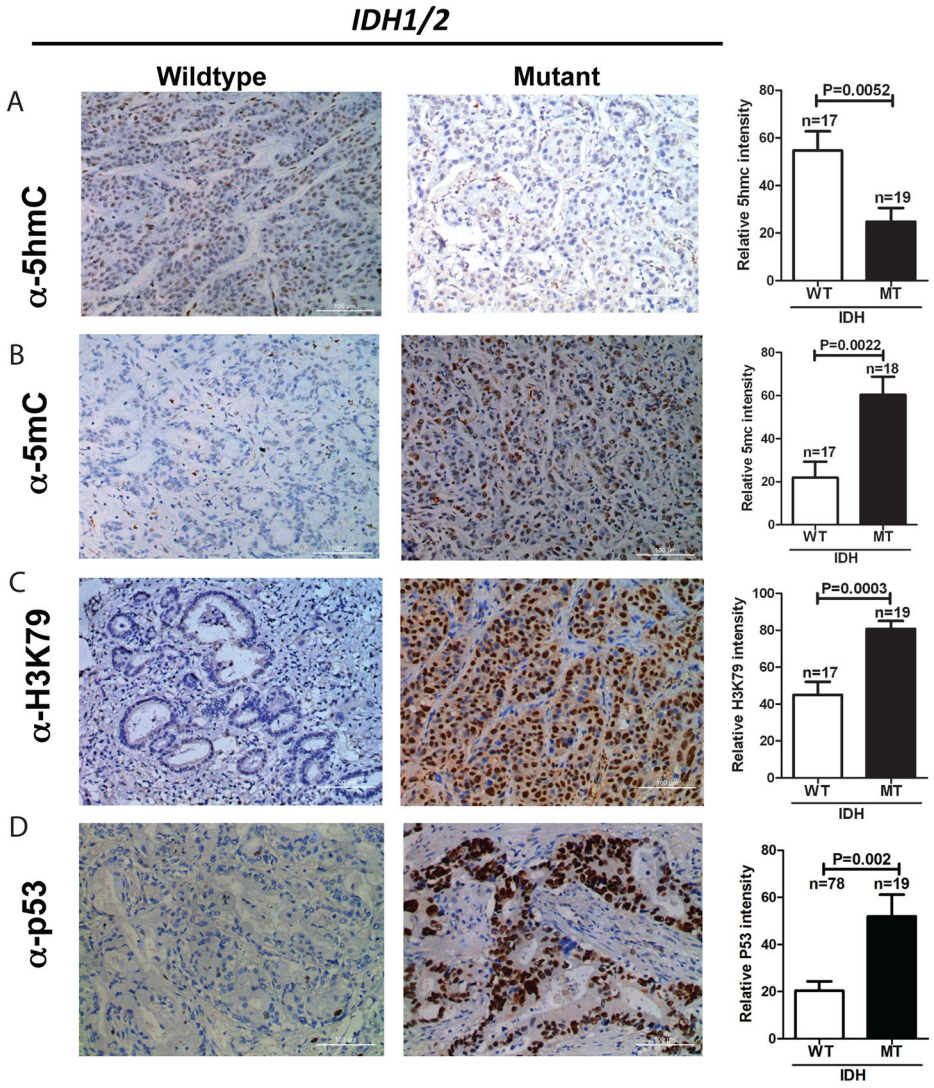

Figure 2. Biochemical effects of *IDH1* and *IDH2* mutations in cholangiocarcinomas

Immunohistochemistry of (A) 5-hydroxymethylcytosine, (B) 5-methylcytosine, (C) histone H3K79 dimethylation, and (D) p53. Representative tumor samples are shown for cholangiocarcinomas that were wild-type or mutant for *IDH1* or *IDH2* (left panel). Scale bars represent 100μm. In the right panel, the average positive area across 17 *IDH1/2* wild-type, or 19 *IDH1/2* mutant, cholangiocarcinomas are shown. For p53 staining, 78 IDH1/2 wild-type cholangiocarcinomas were assessed.

Author Manuscript Author Manuscript Author Manuscript Author Manuscript

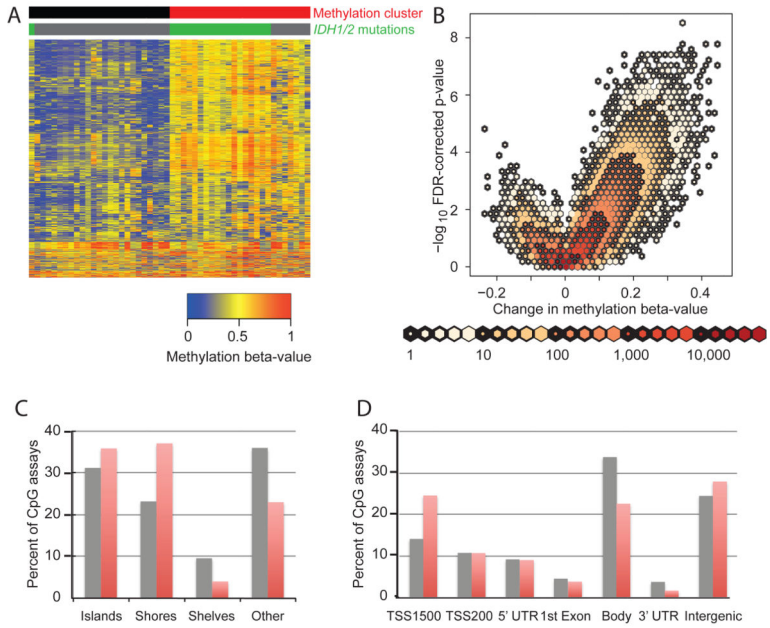

Figure 3. Cholangiocarcinomas with *IDH1* or *IDH2* mutations are associated with increased DNA methylation

(A) Consensus hierarchical clustering of 50 intrahepatic cholangiocarcinomas. Each row depicts the methylation beta-value for a single CpG assay, ranging from 0 (blue) to 1 (red). The sample columns are ordered by the frequency of sample pair co-occurrence in 500 re-samplings of K-means clustering, while re-sampling 4,000 of the CpG sites and 80% of the tumors. Tumors with *IDH1* or *IDH2* mutations are denoted by green bars.

(B) Volcano plot demonstrates association of *IDH1* or *IDH2* mutation with increased methylation. Each dot represents one of the 462,732 CpG sites assayed on the HumanMethylation450 Beadchip. The difference in methylation beta-value between the average of 12 tumors with *IDH1* or *IDH2* mutations and the average of 28 tumors without mutations is plotted on the horizontal axis. The FDR-adjusted *p*-values from a *T* test are plotted on the vertical axis.

(C) Enrichment of hypermethylated CpG sites relative to annotated CpG islands. Histograms of CpG sites associated with increased methylation in tumors with *IDH1* or *IDH2* mutations, as annotated by the relative position to CpG islands in the UCSC annotation. The frequency of annotation categories is compared between 5,189 hypermethylated CpG sites (red bars) and the 462,732 CpG sites on the array (grey bars).

(D) Enrichment of hypermethylated CpG sites relative to annotated coding regions. The same as (C), using annotations relative to Refseq transcripts.

Author Manuscript Author Manuscript Author Manuscript Author Manuscript

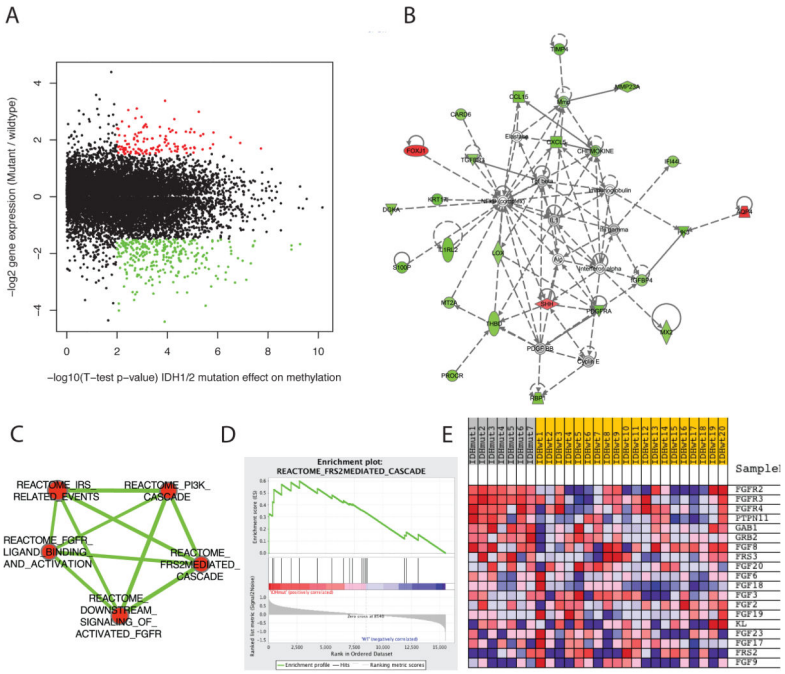

Figure 4. Gene expression consequences of *IDH1* or *IDH2* mutations in cholangiocarcinomas

(A) Starburst plot of DNA methylation versus gene expression. Each point represents a CpG assay annotated in the 1500 bp upstream of transcription start sites, along with the gene expression difference between 7 *IDH1* or *IDH2* mutant cholangiocarcinomas and 20 *IDH1* or *IDH2* wild-type cholangiocarcinomas. Hypermethylated CpG sites with significant decreases in gene expression are highlighted in green. Genes with >2.8-fold increases in gene expression are highlighted in red.

(B) Ingenuity Pathway Analysis of the top-scoring network among 285 down-regulated and hypermethylated genes.

(C) Gene Set Enrichment Analysis (GSEA) of overexpressed genes in cholangiocarcinomas with *IDH1* or *IDH2* mutations. Green lines indicate gene set annotation pairs share at least 50% of genes.

(D) Representative GSEA enrichment plot for FRS2-mediated signaling cascade.

(E) Expression levels of genes annotated in FRS2-mediated signaling cascade. Red indicates upregulated genes, and blue indicates downregulated genes. Each row represents a gene, and each column indicates a cholangiocarcinoma with *IDH1* or *IDH2* mutation (grey) or without mutations (orange).

Author Manuscript Author Manuscript Author Manuscript Author Manuscript

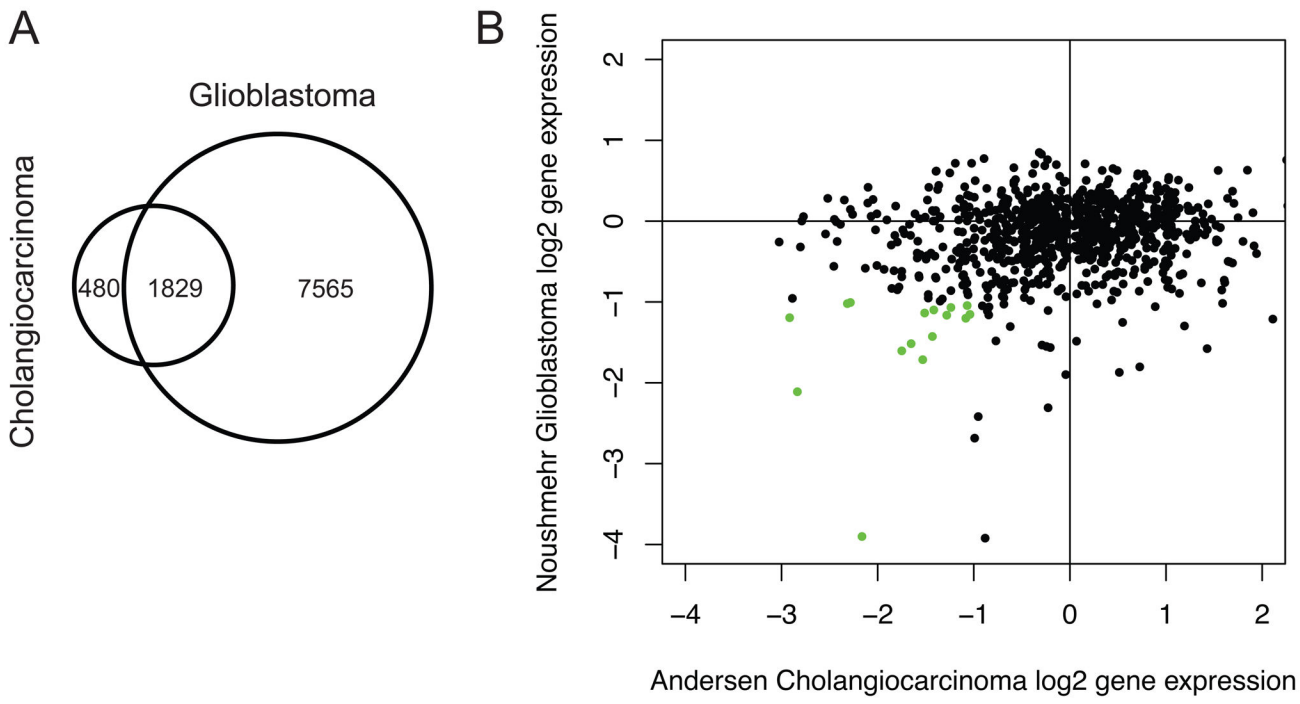

Figure 5. Common methylated targets in *IDH1/2*-mutated cholangiocarcinomas and glioblastomas

(A) Venn diagram of overlapping hypermethylated genes between *IDH1/2*-mutated cholangiocarcinomas and *IDH1*-mutated glioblastomas.

(B) Gene expression consequences of commonly methylated genes. Microarray data is shown as log2 fold change between 7 *IDH1/2*-mutated and 20 *IDH1/2*-wild-type cholangiocarcinomas (32) (horizontal axis), as well as log2 fold change between 21 G-CIMP-positive and 52 G-CIMP-negative proneural glioblastomas (15) (vertical axis).

Author Manuscript Author Manuscript Author Manuscript Author Manuscript

Oncogene. Author manuscript; available in PMC 2013 December 20.

Table 1

Mutations of *IDH1*, *IDH2*, *KRAS* and *TP53* in intrahepatic cholangiocarcinoma

Sample ID	Mutant gene	Nucleotide change	Amino acid change	Allele frequency	KRAS Codon 12/13	TP53 exons 4–9
03-414	IDH1	ATA -> ATG	I99M		WT	WT
03-110	IDH1	CGT -> TGT	R132C	25%	WT	WT
06-284	IDH1	CGT -> TGT	R132C	38%	G12R	WT
06-585	IDH1	CGT -> TGT	R132C	25%	G12D	R213stop
07-078	IDH1	CGT -> TGT	R132C	40%	WT	WT
07-138	IDH1	CGT -> TGT	R132C	37%	WT	WT
07-258	IDH1	CGT -> TGT	R132C	30%	WT	WT
08-28059	IDH1	CGT -> TGT	R132C		WT	
07-25379	IDH1	CGT -> TGT	R132C		WT	
98-2018B	IDH1	CGT -> TGT	R132C		WT	
6288T	IDH1	CGT -> TGT	R132C		WT	
03-447	IDH1	CGT -> GGT	R132G		G13D	WT
05-207	IDH1	CGT -> GGT	R132G		G12D	WT
08-137	IDH1	CGT-> CTT	R132L	28%	WT	WT
07-15695	IDH1	CGT -> CTT	R132L		WT	
CC002T	IDH1	CGT -> GGT	R132G		WT	
CC003T	IDH1	CGT -> GGT	R132G		WT	
CC019T	IDH1	CGT -> TGT	R132C		WT	
CC026T	IDH1	CGT -> GGT	R132G		WT	
CC047T	IDH1	CGT -> TGT	R132C		WT	
CC013	IDH1	CGT -> AGT	R132S		WT	
CC028	IDH1	CGT -> GGT	R132G		Q61H	
CC032	IDH1	CGT -> GGT	R132G		WT	
03-184	IDH2	AGG -> AAG	R172K		WT	WT
08-58989	IDH2	AGG -> AAG	R172K		WT	
07-141	IDH2	AGG -> AAT	R172N		WT	
04-129	IDH2	AGG -> TGG	R172W		WT	WT
07-255	IDH2	AGG -> TGG	R172W		WT	WT

Author Manuscript Author Manuscript Author Manuscript Author Manuscript

Sample ID	Mutant gene	Nucleotide change	Amino acid change	Allele frequency	KRAS Codon 12/13	TP53 exons 4–9
07-52956	IDH2	AGG -> TGG	R172W		WT	
08-29844	IDH2	AGG -> TGG	R172W		WT	
5850	IDH2	AGG -> AAG	R172K		WT	
CC043	IDH2	AGG -> TGG	R172W		WT	
CC045	IDH2	AGG -> AAG	R172K		WT	
100550	IDH2	AGG -> AAG	R172K			
05-293	KRAS				G12D	
05-484	KRAS				G12D	
07-009	KRAS				G12D	
06-170	KRAS				G12A	
07-237	KRAS				G12A	
03-128	KRAS				G12C	
05-275	KRAS				G12C	
03-040	KRAS				G13D	

Author Manuscript Author Manuscript Author Manuscript Author Manuscript

Table 2

Univariate and multivariate analyses of factors associated with time to recurrence of intrahepatic cholangiocarcinoma (N = 252)

Variable	Univariate analysis			Multivariate analysis		
	HR	95% CI	*P value*	HR	95% CI	*P value*
Sex (Male vs. Female)	0.833	0.584–1.189	0.315	n.a.		
Age (>55 vs. ≤55)	1.017	0.714–1.448	0.925	n.a.		
HBsAg (+ vs. −)	0.921	0.632–1.341	0.667	n.a.		
Tumor size, cm (>5 vs. ≤5)	1.643	1.126–2.398	0.010	1.631	1.112–2.395	0.012
Tumor number (multiple vs. single)	1.046	0.547–2.000	0.891	n.a.		
Encapsulation of tumor (complete vs. none)	2.049	1.097–2.825	0.024	1.838	0.982–3.442	0.057
History of cirrhosis (yes vs. no)	1.089	0.508–2.339	0.826	n.a.		
Portal lymph node invasion (yes vs. no)	1.804	1.210–2.691	0.004	1.621	1.078–2.438	0.020
Tumor differentiation (III~IV vs.I~II)	1.346	0.934–1.939	0.111	n.a.		
TNM stage (III vs.I~II)	1.242	0.847–1.819	0.267			
IDH (mutation vs. wild type)	0.512	0.273–0.960	0.037	0.477	0.254–0.894	0.021

Univariate analysis, Cox proportional hazards regression.

Multivariate analysis, Cox proportional hazards regression.

95% CI, 95% confidence interval.

Tumor differentiation was assigned by Edmondson’s grading system

n.a., not applicable: Variable was not used in the multivariate Cox regression model

Oncogene. Author manuscript; available in PMC 2013 December 20.